Estuarine, Coastal and Shelf Science (1999) **49,** 483–499
Article No. ecss.1999.0520, available online at http://www.idealibrary.com on IDEAL®

Lateral Transport of Lithogenic Particles from the Continental Margin of the Southern East China Sea

J. J. Hung, C. S. Lin, G. W. Hung and Y. C. Chung

Institute of Marine Geology and Chemistry, National Sun Yat-Sen University, Kaohsiung, Taiwan, R.O.C.

Geochemical compositions and fluxes of suspended and trapped (settling) particulate matter were studied to elucidate particle sources and transports from the continental margin of southern East China Sea (ECS) to the Okinawa Trough. Experimental results indicate that the abundance of suspended particulate matter (SPM) and lithogenic elements (Al, Fe and Mn) decreases with an increase of distance from the land, but increases with water depth, implying the resuspension and lateral transport of SPM over the southern ECS shelf and upper slope. This transport process is further demonstrated by a decrease of mass flux from the Mien-Hwa Canyon (MHC) to the Okinawa Trough, but an increase of mass flux with depth for trapped particulate matter (TPM). In addition, mass fluxes are anomalously high and substantially greater within the MHC (6·64–71·5 g m^{-2} day^{-1}) than nearby slope areas (0·77–15·7 g m^{-2} day^{-1}) and other globally analogous environments. MHC appears to function as an essential conduit for particle transport. Both SPM and TPM collected below the surface layer are mainly lithogenic. Approximately 76·2–89·3% of TPM are lithogenic materials regardless of trap sites, strongly indicating that laterally lithogenic sources must add to vertical mass fluxes across the margin. Biogenic contributions are relatively small, ranging from 1·05 to 6·54% for organic matter, from 6·33 to 14·3% for carbonate and from 0·67 to 3·50% for opal, resulting from dilution by lithogenic materials. Vertical fluxes may just contribute 8–34% of Corg fluxes collected from bottom traps. Statistical correlations among Al, K, Mn, Mg and Fe contents are highly significant, also reflecting that TPM is primarily lithogenic. However, only 40–73% of collected TPM may be regarded as recent inputs from the Yangtze River. Particles resuspended and advected from shelf and/or slope may contribute significantly to TPM collected between the upper slope and the Okinawa Trough. Furthermore, short-term variabilities of mass and lithogenic fluxes on all trap occupations may arise from episodic events of resuspension/lateral transport, rather than from temporal variations of riverine inputs and local production.

Keywords: suspended particulate matter; sediment traps; geochemistry; South China Sea; sediment transport; Taiwan

Introduction

The East China Sea (ECS) is one of the largest marginal seas worldwide, receiving enormous rates of fresh water (>885 km^3 yr^{-1}) and suspended sediment (>1·4 × 10^9 tons yr^{-1}) from Yangtze (Changjiang) and Yellow (Huangho) Rivers (Milliman & Meade, 1983). The relatively wide ECS continental shelf can potentially retain sediment emptied from the rivers. However, previous investigations have indicated that suspended sediment particularly that discharged from the Yangtze River is only slightly transported offshore in an easterly and north-easterly direction. Although deposited in the estuary and near the river mouth during flood seasons, most sediment is resuspended by subsequent winter storms and transported southward by a coastal current (Chin, 1979; Milliman *et al.*, 1985; Sternberg *et al.*, 1985). This transport mode is likely related to the present texture of sediment in middle and outer shelves occupied largely by relict sand (Chin, 1979).

The southward sediment carried by the relatively turbid China coastal water (CCW) has obviously not ended up in the Taiwan Strait (Li, 1994). The southward-flowing CCW turns cyclonically in the northern Taiwan Strait, resulting from blockage by a topographic high as well the northward Kuroshio branching current (Chao, 1991; Jan, 1995). Therefore, we can infer that the CCW may eventually carry suspended sediment southwards across the shelf off northern Taiwan and empty it largely into the Okinawa Trough. Meanwhile, this seaward flux of suspended sediment may be augmented by proximity to sources from northern Taiwan, although the annual loading of riverine SPM from northern Taiwan (*c.* 2 × 10^7 ton yr^{-1}) is much smaller than those from Yangtze and Yellow Rivers.

Submarine canyons are important conduits for transferring modern sediment from the shelf to the deep sea during high stands of sea level (Baker & Hickey, 1986; Thorbjarnarson *et al.*, 1986; Gardner, 1989). The Mien-Hwa Canyon (MHC) and the North Mien-Hwa Canyon (NMHC) are two major submarine canyons off north-eastern Taiwan, incising across the southern ECS slope onto the Okinawa Trough. On the eastern side of shelf break, the Kuroshio Current which begins east of Luzon and passes the east coast of Taiwan, flows north-eastward

0272–7714/99/100483+17 $30.00/0

and impinges on the continental shelf off north-eastern Taiwan. A branch of the Kuroshio turns north-westward along the NMHC and intrudes onto the shelf before the mainstream continues to flow into the north Pacific Ocean (Nitani, 1972; Chern *et al.*, 1990; Hsueh *et al.*, 1992; Tang *et al.*, 1999). Meanwhile, a south-westward countercurrent branches off from the Kuroshio Subsurface Water spreading to the slope (Chung *et al.*, 1993), thereby feeding the year-round upwelling around the shelf break covering the area of MHC head (Liu *et al.*, 1992). Intensive mixing and exchange among the upwelled water, intruded Kuroshio water and shelf waters occurred in this study area. Consequently, a major portion of upwelled countercurrent may merge with shelf mixed water and outflow through the Mien-Hwa Canyon (Tang *et al.*, 1999), possibly facilitating the particle transport as well. Therefore, this study investigates the geochemical characteristics of suspended particulates collected from a transect between the China coast and the South Okinawa Trough as well as particles collected from sediment traps deployed between the southern ECS slope and the South Okinawa Trough. By doing so, the source and transport of particulate matter from the ECS shelf and slope to the Okinawa Trough is elucidated.

Sampling and analytical methods

The TPM samples were collected with French-made time-series sediment traps (TECNICAP P.P.S. 3/3) delineated previously by Heussner *et al.* (1990). The cylindrical trap, including a carousel with twelve plastic collection cups, has an aspect ratio of 2·5 and a collecting area of 0·125 m^2. The deployment and recovery of sediment traps and the pre-treatment of collected sediment are described elsewhere (Hung & Chung, 1998). Figure 1 illustrates nine arrays (T1–T6; T8–T10) of sediment traps deployed, respectively, in the MHC (T1–T3), along the outlet of MHC to the Okinawa Trough (T4–T6), in the south-west of MHC (T8), on the slope between the MHC and NMHC (T9) and on the slope near the NMHC (T10). Table 1 lists the deployed duration and depths of each sediment trap as well as the water depth of each deployed site. The recovered TPM was wet-sieved through 1 mm nylon mesh to remove large organisms and then, divided into subsamples by a perimatic dispenser (Hung & Chung, 1998). Each split subsample used herein was filtered with a pre-weighed 47 mm Nucleopore filter (0·4 μm) and then, washed with DDW to remove the remaining sea salt and formalin solution used to TPM preservation during collection and storage. Next, the washed sample was dried in an oven at 60 °C and re-weighed to determine the mass flux. The dried samples were then separated from the filter and ground for analyses of major constituents and chemical fluxes. In addition, an aliquot of intact TPM was used for particle size analyses (Counter LS Particle Size Analyzer).

Total organic carbon (TOC) was analysed by placing 20–30 mg TPM in a silver cup and adding a few drops of 2 M HCl to remove carbonate. The acidified sample was dried in an oven and then determined with a C/N/S analyser (Fisons NCS 1500). Another portion of TPM without acid treatment was used for total carbon (TC) analyses. Organic matter content was assumed to be twice TOC (Gordon, 1970; Monaco *et al.*, 1990). Carbonate content was calculated by multiplying inorganic carbon (difference between TC and TOC) by 8·33 (Monaco *et al.*, 1990). Biogenic opal was determined using a colorimetric method modified from that of Mortlock and Froehlich (1989). Briefly, the sample was subsequently treated with acetic acid (pH 5) and H_2O_2 (2%) to remove carbonate and organic matter. Apparent biogenic Si was extracted with 0·5 M NaOH at 85 °C for 5 h, and then, determined colorimetrically. Non-biogenic Si was estimated from extracted Al determined with flameless atomic absorption spectrometry (Perkin-Elmer 5100PC HGA-600). Biogenic opal was then estimated by substracting non-biogenic Si from apparent biogenic Si (Leinen, 1977).

To analyse particulate elements, an exact amount (*c.* 0·2 g) of ground TPM was weighed into a Teflon bottle digested with mixed super-pure acids (HNO_3:HCl:HF=3:3:4) and heated stepwise (stage 1: 420 W, 30 min; stage 2: 600 W, 60 min) by a microwave (CEM 2000). The digested solution was diluted with Q-H_2O and then used to measure Al, Fe, Mn, Mg, and K with atomic absorption spectrometry. Aluminosilicate abundance was estimated from particulate Al (Al/0·0823). Lithogenic materials were calculated by substracting organic matter, carbonate and opal from the total mass. Fluxes of major constituents were estimated from mass fluxes and contents of major constituents.

Suspended particulate matter was collected on a membrane filter by filtration on board the RV *Ocean Researcher I* during ORI-352B 21–28 April 1993) and ORI-405C 6–12 November 1994) cruises. Figure 1 shows the visited stations in a transect across the southern ECS shelf and slope. To determine SPM contents, seawater samples were retrieved with 20-l Go-flo bottles mounted on a CTD/Rosette which recorded the temperature and salinity profiles as well. The Go-flo bottles were thoroughly cleaned with

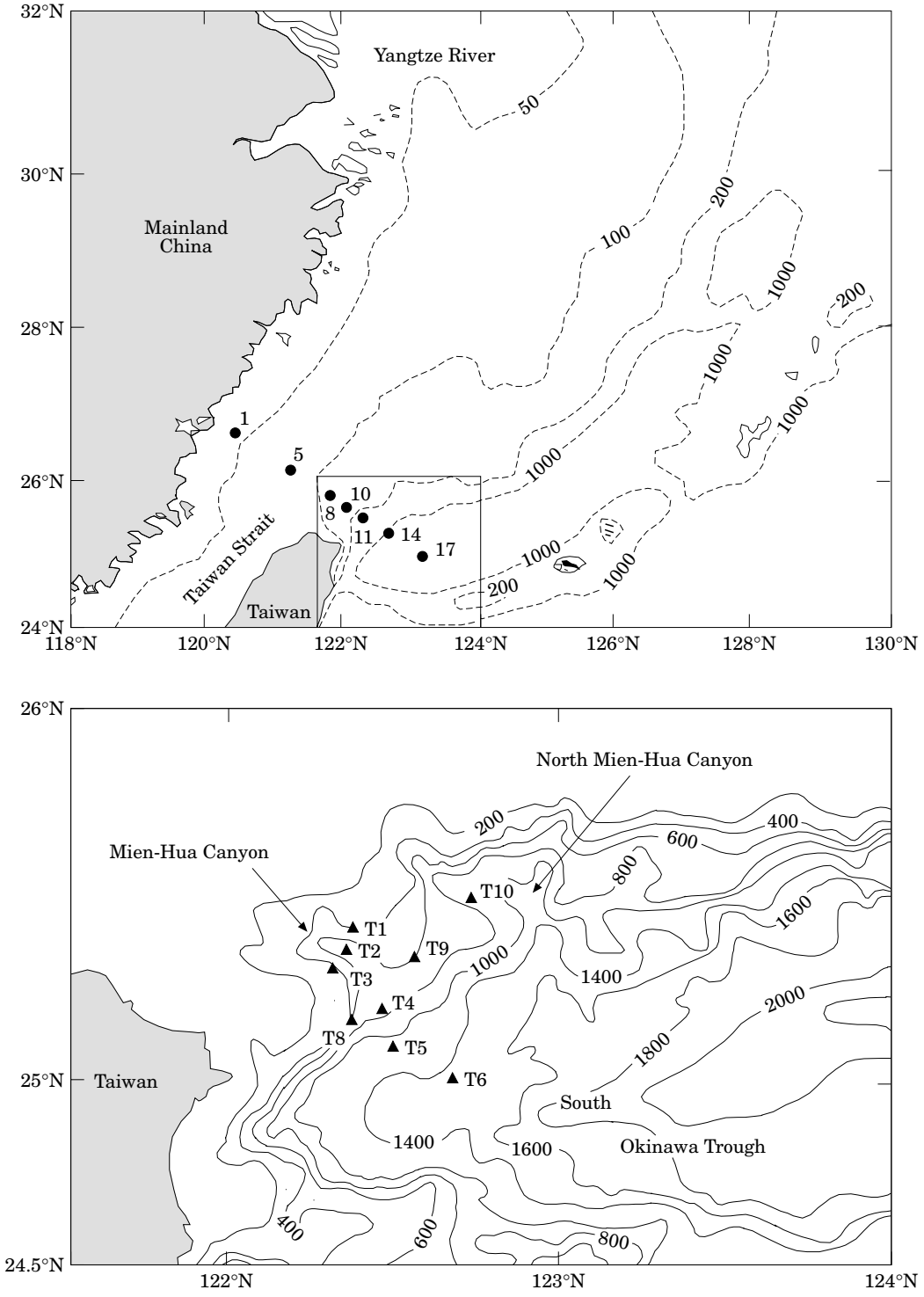

FIGURE 1. Maps displaying the sampling locations of suspended particulate matter (upper figure, St. 1–St. 17) and settling particulate matter collected with sediment traps (lower figure, T1–T10 trap sites).

diluted acid and distilled-deionized water (DDW) before the cruise. After draining the recovered seawater into acid-cleaned PE containers (20 l), the water sample was filtered through an acid-cleaned and pre-weighed Nucleopore membrane filter (142 mm, 0·4 μm pore size) driven by a peristaltic pump and a silicone tube connected to a Teflon filter holder. The total volume of seawater to be filtered ranging from

TABLE 1. Locations, water depths, moored depths, sampling interval and deployment periods set for sediment traps and associated current meters in this study

Trap site	Location N	Location E	Water depth (m)	Moored depth (m) height (mab) Trap	Moored depth (m) height (mab) Current meter	Sampling interval (days)	Prevailing current direction	Mean speed (cm s^{-1})	Deployment period
T1	25°25′	122°21′	490	325 (165)	330 (160)	3	SWW	5	27/10–1/12/92
				407 (83)	412 (78)		NW	5	
T2	25°22.4′	122°19.1′	695	[404]	409 (286)	5, 6	NE	7	31/3–4/6/92
				606 (89)	611 (84)		W	5	
T3	25°20.4′	122°17.9′	578	[278]	328 (250)	8	SW	10	21/7–25/10/93
				378 (200)			—	—	
				528 (50)	533 (45)		SW	5	
T4	25°12.6′	122°28′	818	[290]		10	—	—	10/11/93–9/3/94
				390 (428)	395 (423)		SES	20	
				490 (328)			—	—	
				590 (228)	595 (223)		SW	10	
T5	25°6.5′	122°30.1′	1060	[360]	365 (695)	10	SE	15	5/5–1/9/94
				560 (500)	565 (495)		S	10	
				760 (300)	765 (295)		E, S	5	
				960 (100)	965 (95)		—	5	
T6	24°59.6′	122°39.3′	1446	746 (700)	896 (550)	15	S	5	14/11/94–12/5/95
				[1046]	1196 (250)		SE	3	
				1346 (100)			—	—	
T8	25°10.1′	122°22.1′	605	355 (250)	360 (245)	13	—	5	13/7–15/12/95
				505 (100)	510 (95)		SW	7	
T9	25°20.2′	122°32.9′	607	407 (200)	412 (195)	13	SWS	12	13/7–15/12/95
				507 (100)	512 (95)		SWS	8	
T10	25°30′	122°43′	1006	[306]		13	—	—	13/7–15/12/95
				606 (400)	611 (395)		SW	5	
				906 (100)	911 (95)		SWW	3	

Notes: [ ] indicates malfunction of instrument; ( ) indicates metres above bottom (mab).

15 to 40 l, depending on the content of suspended particulate matter. The filter's residue was then washed with 500 ml DDW to remove the remaining sea salt. Finally, the filters were dried in an oven at 60 °C and re-weighed with a microbalance (Mettler AT20) to determine SPM contents in seawater.

Geochemical composition of SPM was analysed by digesting the filtered residue with mixed super-pure acids and determined either with flame or flameless atomic absorption spectrometry according to the procedures described above for TPM. However, particulate organic carbon (POC) and nitrogen (PN) were determined by filtering SPM on a GF/F filter. Finally, the filtered SPM was acidified to remove carbonate and then measured for POC and PN with a Fisons C/N/S Analyzer.

Results and discussion

Distribution and transport of suspended particulate matter

According to distributions of temperature and salinity, at least four types of water can be identified across a transect from the China coast to the South Okinawa Trough (Figure 2). They were China coastal water (CCW, St. 1), Taiwan current warm water (TCWW, St. 5), upwelled water (UW, Sts. 8–11) and Kuroshio water (KW, St. 17). The CCW was characterized by low temperature and salinity as well as a heavy load of SPM, which was apparently influenced by the runoff from the Yangtze River. Although having a relatively uniform temperature and salinity, the TCWW had various SPM with depth, reflecting the characteristic of northward Taiwan Strait water. The UW was upwelled primarily from Kuroshio subsurface water and mixed with ECS shelf water. Therefore, the temperature and salinity of UW generally converged at 15 °C and 34·6, respectively. Notably, the SPM distribution becomes less variable with depth beyond the shelf break. The KW was characterized by a high temperature and salinity, but low SPM. The striking reversed S-shape in the T-S diagram (Figure 2) displays a maximum salinity >34·7. This salinity maximum was also found in the North Pacific subtropical water (Nitani, 1972).

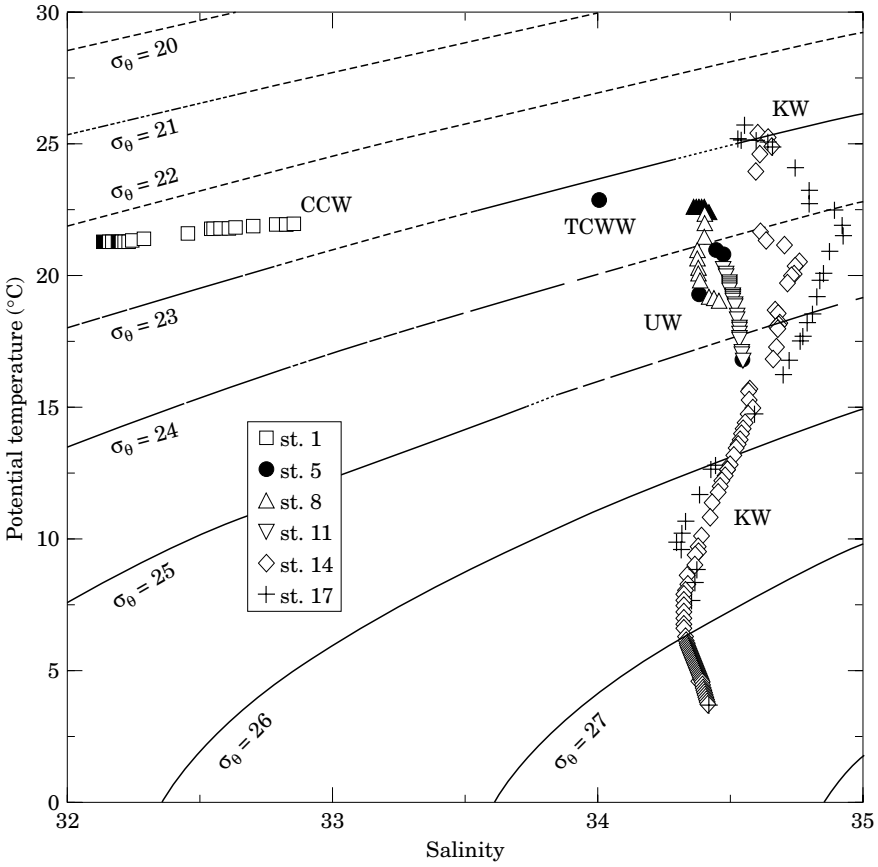

FIGURE 2. Temperature–salinity plots for sampling locations from the Cruise 405C.

Southern ECS shelf water is more turbid than slope water (Figure 3). The SPM profile reveals that although decreasing seaward, SPM contents dramatically increase downward in the shelf and upper slope areas in both spring (Cruise 352B) and autumn (Cruise 405C) seasons. The SPM variations between the onset of south-west (spring) and the onset of north-east (autumn) prevailing monsoon seasons may arise from changes in biological productivity and physical forcing. The seaward decrease of SPM may result from the decrease of biological productivity and terrestrial source, while the SPM in the shelf region downwardly increases owing primarily to the resuspension of local and/or remote bottom sediment caused by strong wind-induced mixing and tidal fluctuation. For instance, in the 405C cruise, SPM increased up to 5-fold near the bottom of Station 1 when the wind speed was 15 m s^{-1}. Meanwhile, the current velocity and SPM measured from 60 m depth (15 m above bottom) at Station 7 of the same transect during late August 1993 reveal that SPM concentrations were markedly greater in the period with eastward current than in the period with westward current. The averaged SPM concentration was 2·80 mg l^{-1} in the eastward-current period and 1·57 mg l^{-1} in the westward-current period. Bottom SPM was apparently transported seaward as water moved offshore. The resuspension dramatically reduces as the location shifts away from the shelf break probably due to a quiescent condition of deeper environment. This lateral transport enhanced by bottom resuspension can also be verified by TPM flux data in which the deeper mass fluxes are always greater than those upper ones (Figure 5). SPM concentration below the euphotic layer appears to be greater in the MHC-axis transect than in northern non-canyon area reported by Hung and Chan (1998), although the latter was obtained during a different season. A relatively turbid water was found in the intermediate layer (500–800 m) of deep slope water at Station 17 [Figure 4(a)] which may be derived from the detached bottom sediment transported away from the slope, particularly from the canyon slope. A similar phenomenon has also been observed in canyon-axis slopes from American east (Gardner, 1989) and west coasts (Drake, 1974; Baker, 1976).

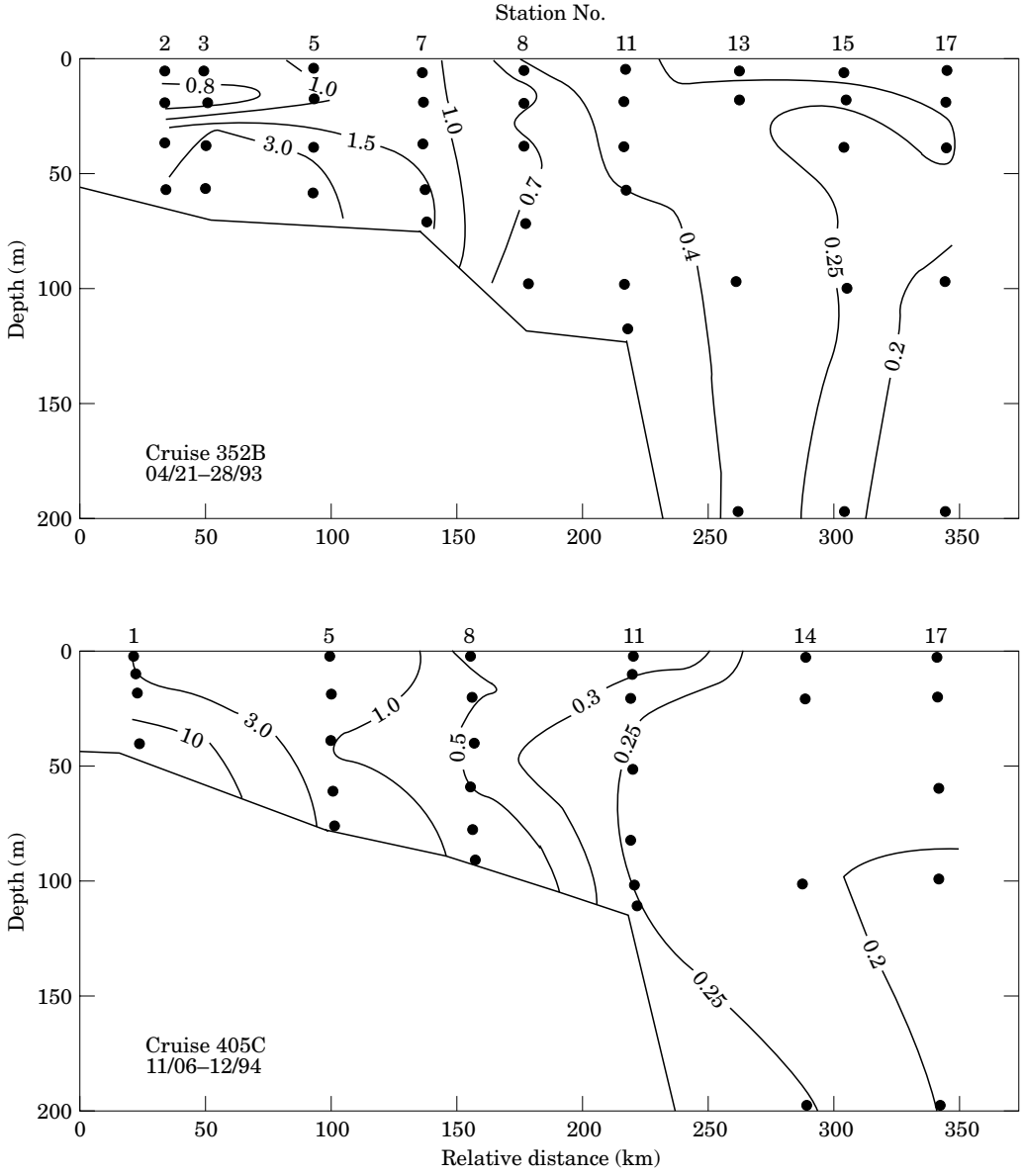

FIGURE 3. SPM distributions (mg l^{-1}) along the cross-shelf transect observed from 352B and 405C cruises.

MHC appears to function as an essential conduit for sediment transport.

Geochemical transport of suspended particulate matter

Table 2 lists the geochemical composition of SPM in the transect of ORI-405C cruise. Although POC content (μg l^{-1}) in seawater decreases seaward, its concentration in SPM (%) generally increases seaward. This distribution pattern is also true for PN. Apparently, the contribution of biogenic organic matter to SPM increases seaward, particularly for the euphotic zone of UW and its flanked waters. In contrast, aluminium, i.e. a lithogenic element, decreases seaward both content in seawater and concentration in SPM. Aluminium content and concentration also increase with the increase of water depth. The concentration of Al in near bottom SPM is close to the Al concentration in sediment over the inner shelf (data not shown here); reflecting the sediment resuspension which was also referred from SPM distributions mentioned earlier. Aluminosilicate estimated from Al content is the predominant component of SPM in southern ECS shelf except for the euphotic layer of UW (Sts. 8 and 11). Notably, distributions and transport patterns of particulate Fe and Mn

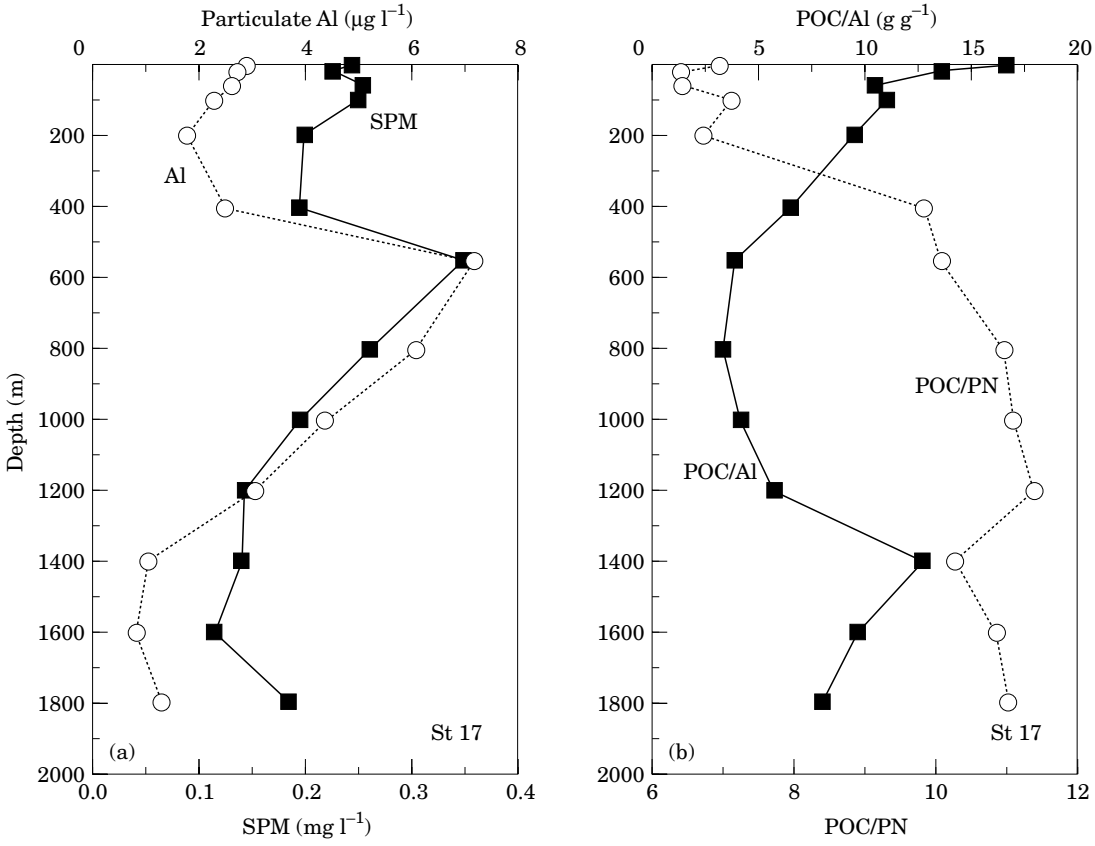

FIGURE 4. Vertical distributions of SPM and particulate Al (A) and distributions of POC/Al and POC/PN ratios (B), showing characteristics of an intermediate layer plume between 550 and 800 m at Station 17.

TABLE 2. Geochemical composition of SPM in water columns of ORI-405C transact

	St. 1	St. 5	St. 8	St. 11	St. 14	St. 17
SPM (mg l^{-1})	2·96– 20·6	0·91–2·68	0·31–0·87	0·20–0·35	0·20–0·27	0·12–0·27
Org C (μg l^{-1})	115–386	49·6–82·7	39·9–130	45·0–75·5	28·1–61·8	8·40–48·7
Org C (%)	1·87–5·00	3·07–5·46	4·60–30·2	18·0–30·3	11·2–27·2	6·07–19·5
Org N (μg l^{-1})	18·3–55·7	8·33–11·2	5·10–22·6	8·22–15·4	3·09–9·80	0·90–8·13
C/N (euphotic zone)	7·42–7·86	6·65–7·66	6·63–7·60	5·43–6·75	7·21–7·50	6·46–7·14
(aphotic zone)	7·44–8·15	7·22–8·87	7·85–9·15	6·30–6·63	9·10–10·6	9·87–11·4
Al (μg l^{-1})	142–1465	29·6–96·8	3·76–39·6	3·78–11·1	0·47–10·2	0·83–7·15
Al (%)	3·83–6·74	1·60–96·8	3·76–39·6	3·78–11·1	0·47–10·2	0·83–7·15
Aluminosilicate (%)	46·5–81·9	19·4–70·2	14·8–49·7	18·1–61·2	1·12–45·2	2·61–32·1
Fe (μg l^{-1})	88·2–717	78·8–134	3·72–30·0	3·76–8·46	3·74–10·4	2·96–12·0
Mn (μg l^{-1})	1·8–19·1	0·97–2·25	0·11–0·33	0·12–1·32	0·29–2·20	0·27–2·70

resemble those of particulate Al, implying that SPM is largely lithogenic in the water below the euphotic layer over the shelf region.

Bottom resuspension contributes significantly to the formation of benthic nepheloid layer in the shelf (Figure 3), which is likely to be a major pathway in transport of SPM and lithogenic elements from the shelf to the slope. Vertical distributions of particulate Al [Figure 4(a)] in slope water (St. 17) strongly support the presence of intermediate nepheloid layer (INL) described above from SPM distributions. Wei *et al.* (1991) first reported on a similar plume from a nearby station by measuring the total Mn extractable by Chelex-100 resin based on a single cruise. Hsiung

TABLE 3. Fluxes (mg m^{-2} day^{-1}) and contents (%) of total mass and chemical constituents from sediment traps moored at T1 to T10

Traps site	Depth (m)	Mean mass flux	Organic matter		Opal		Carbonate		Aluminosilicate[a]		Lithogenic[b]	
			F	%	F	%	F	%	F	%	F	%
T1	325 m, 165 mab	33 100	390	1·34	195	0·67	3457	10·1	14 130	42·7	29 130	88·0
	407 m, 83 mab	57 830	730	1·35	420	0·80	5573	9·54	23 720	41·0	51 180	88·4
T2	606 m, 89 mab	54 820	434	1·05	250	0·76	5248	9·35	29 170	57·0	48 880	88·8
T3	378 m, 200 mab	6640	100	1·81	91	1·63	675	10·4	3720	56·4	5780	86·2
	528 m, 50 mab	71510	736	1·26	755	1·28	6248	8·68	41 160	60·5	63 770	88·8
T4	390 m, 428 mab	4040	78	2·44	37	1·04	342	8·34	2670	67·1	3580	88·2
	490 m, 328 mab	6380	108	1·95	65	1·24	533	8·18	4220	67·9	5670	88·6
	590 m, 228 mab	9900	160	1·71	139	1·47	858	8·34	6190	62·9	8750	88·5
T5	560 m, 500 mab	5750	140	2·98	131	2·96	375	6·33	4140	72·7	5480	87·7
	760 m, 300 mab	7740	178	2·56	151	2·47	558	7·23	5690	75·0	6850	87·7
	960 m, 100 mab	15 730	200	1·96	229	1·87	1483	7·71	11 210	74·1	13 820	88·5
T6	740 m, 700 mab	3240	78	2·42	44	1·33	225	6·94	2110	64·9	2900	89·3
	1340 m, 100 mab	4980	116	2·36	72	1·26	333	6·63	3350	66·8	4460	89·8
T8	355 m, 250 mab	16 380	238	1·70	153	1·19	1474	8·91	9330	58·6	14 510	88·2
	505 m, 100 mab	43 470	588	1·45	377	0·96	3932	9·02	24 690	57·5	38 570	88·6
T9	407 m, 200 mab	770	42	6·53	21	3·04	100	14·3	450	54·3	610	76·2
	507 m, 100 mab	2940	72	3·03	47	2·33	300	10·8	1610	56·5	2530	83·9
T10	606 m, 400 mab	1170	52	4·45	44	3·50	133	11·1	880	74·6	940	80·9
	906 m, 100 mab	11 890	242	2·10	248	2·24	1208	10·5	8220	70·8	10 190	85·8

[a]Aluminosilicate (%) = Al (%)/0·0823.
[b]Lithogenic flux = mass flux − (organic flux + opal flux + carbonate flux) = (aluminosilicate flux) + (non-aluminosilicate silicic flux).
Lithogenic (%) = 100% − (% organic matter + % opal + % carbonate).
mab: metres above bottom.

et al. (1998) also repeatedly observed the mid-depth plume of dissolved Mn in the same location of Station 17. Particles in the INL is enriched with lithogenic materials (POC<8%) with minimum POC/Al ratios in the water column [Figure 4(b)]. Sherrell *et al.* (1998) reported a positive correlation between $^{14}C_{org}$ and POC/Al (depleted $^{14}C_{org}$ *vs* low POC/Al) in north-east Pacific water columns. They proposed that Al-associated old carbon may be derived either from advected sedimentary material tightly associated with minerals or from the exchange of old DOC with sedimentary carbon after resuspension. Apparently, POC in the INL is relatively old and likely derived from slope sediment if Sherrell's findings can be widely applicable. This mid-depth plume not only provides the major pathway for exporting substances from the shelf to the deep ocean, but also can be important in facilitating boundary scavenging of particle-reactive trace elements supported by the enrichment of Mn in TPM collected from trap 6 (Table 4).

Spatial variability of total mass and chemical fluxes

Table 3 lists and Figure 5 partially replots the total mass fluxes and major chemical composition of particles collected from traps. Total mass and chemical fluxes of each trap are averaged from successful cups set for the sampling interval. Although most traps are deployed on different intervals, spatial variability was quite distinct in fluxes of total mass and chemical constituents among the moored traps. Mass fluxes from T1 (33·1–57·8 g m^{-2} day^{-1}) to T3 (6·64–71·5 g m^{-2} day^{-1}) in the MHC are substantially higher [except for T3 at 378 m (6·64 g m^{-2} day^{-1})] than those from other sites (0·77–43·5 g m^{-2} day^{-1}), implying that the MHC is a major conduit of particle transport in the study area. Mass fluxes from T8 (16·4–43·5 g m^{-2} day^{-1}) are fairly high and comparable with the values measured in the canyon, largely because T8 locates near the canyon outlet and may receive a large portion of particles outfluxed from the canyon and swept toward south-east by the Kuroshio countercurrent. This notion can be supported by a significant decrease (*c.* 80%) of fluxes from the canyon (T1–T3) to middle [T4 (4·04–9·90 g m^{-2} day^{-1})] and deep [T6 (3·24–4·98 g m^{-2} day^{-1})] slopes along the canyon axis, because most particles leaving the canyon are lithogenic (see discussion below) and are not likely to degrade before reaching the T4 site. Mass fluxes are the lowest at T9 (0·77–2·94 g m^{-2} day^{-1}) deployed on the middle

TABLE 4. Elemental concentrations (X_i) and X_i/Al ratios of particles from T1 to T10 traps

Trap site		Al (%)	Trap Al / River Al[a]	Fe (%)	Fe/Al	Mn (%)	Mn/Al (10^{-2})	Mg (%)	Mg/Al	K (%)	K/Al
T1	− 325 m	3·51	0·42	2·66	0·76	0·048	1·36	0·53	0·15	1·72	0·49
	− 407 m	3·38	0·40	2·82	0·83	0·054	1·60	0·53	0·16	1·67	0·49
T2	− 606 m	4·69	0·56	2·38	0·51	0·056	1·19	0·81	0·17	1·68	0·36
T3	− 378 m	4·65	0·55		0·54	0·048	1·03	1·04	0·22	1·67	0·36
	− 528 m	4·98	0·59	2·31	0·46	0·054	1·08	1·11	0·22	1·60	0·32
T4	− 390 m	5·52	0·66	2·70	0·49	0·057	1·03	1·21	0·22	1·88	0·34
	− 490 m	5·59	0·67	2·73	0·49	0·062	1·11	1·27	0·23	1·86	0·33
	− 590 m	5·18	0·62	2·66	0·51	0·059	1·14	1·20	0·23	1·79	0·35
T5	− 560 m	5·99	0·71	2·85	0·48	0·063	1·05	1·25	0·21	1·93	0·32
	− 760 m	6·17	0·73	2·94	0·48	0·068	1·10	1·24	0·20	1·94	0·31
	− 960 m	6·10	0·73	2·84	0·47	0·073	1·20	1·15	0·19	1·91	0·31
T6	− 740 m	5·34	0·64	2·94	0·55	0·063	1·18	1·16	0·22	1·90	0·36
	− 1340 m	5·50	0·65	3·16	0·57	0·126	2·29	1·22	0·22	1·97	0·36
T8	− 355 m	4·82	0·57	2·54	0·53	0·056	1·16	0·53	0·11	1·59	0·33
	− 505 m	4·73	0·56	2·44	0·52	0·060	1·27	0·53	0·11	1·52	0·32
T9	− 407 m	4·47	0·53	2·46	0·55	0·060	1·34	0·92	0·21	1·61	0·36
	− 507 m	4·47	0·53	2·43	0·54	0·063	1·41	0·55	0·12	1·60	0·36
T10	− 606 m	6·14	0·73	2·80	0·46	0·070	1·14	0·46	0·07	1·89	0·31
	− 906 m	5·83	0·69	2·67	0·46	0·090	1·54	0·58	0·10	1·67	0·29
Yangtze River[b] SPM		8·4	—	4·7	—	0·097	—	1·8	—	2·0	—
$(Xi/Al)_{SPM}$		1	—	—	0·56	—	1·16	—	0·21	—	0·24
Yellow River[b] SPM		7·5	—	3·5	—	0·076	—	1·7	—	1·7	—
$(Xi/Al)_{SPM}$		1	—	—	0·47	—	1·01	—	0·23	—	0·23

[a]River Al: 8·4% (taken from Yangtze River); [b]Qu and Yan (1990).

slope between MHC and NMHC, indicating that particle transport may not be significant through the general slope with no canyon. Meanwhile, mass fluxes from T10 (1·17–11·9 g m^{-2} day^{-1}) located on the middle slope of NMHC are significantly lower than those from the MHC. The upward flow of Kuroshio intrusion onto the ECS shelf along the NMHC (Tang *et al.*, 1999) may retard sediment transport through the NMHC. Apparently, NMHC is not as significant as MHC in particle transport from ECS shelf to the Okinawa Trough, although NMHC is geographically larger than MHC. Mass fluxes in this study area are significantly higher than those investigations involving analogous environments such as ECOMARGE-I (0·089–16·2 g m^{-2} day^{-1}) and SEEP (0·052–4·67 g m^{-2} day^{-1}) continental margins (Biscaye *et al.*, 1988; Monaco *et al.*, 1990; Biscaye & Anderson, 1994). The exceptionally high fluxes of this study area may also suggest that the southern ECS slope is a major conveyor belt for sediment transport from ECS shelf to the Okinawa Trough.

There is a downward increase of mass flux at all of the sediment trap sites, particularly for traps on the MHC and T8 (Figure 5). In addition to vertical flux, the horizontal transport of particles must occur to account for a large difference of flux between shallow and deep traps. Particles collected in the study area may originate from continental shelf and slope where the resuspension of bottom sediment occurs episodically. The mean ^{210}Pb flux (9 to 77 dpm cm^{-2} yr^{-1}) measured from the MHC are about 5–40 times the atmospheric flux (~2 dpm cm^{-2} yr^{-1}), indicating additional sources derived laterally (Hung & Chung, 1998). Chung and Chang (1995) reported that ^{210}Pb fluxes (10–26 dpm cm^{-2} yr^{-1}) calculated from inventory in lower-slope sediment were 5–13 times the expected vertical flux (2–3 dpm cm^{-2} yr^{-1}). They strongly suggested that the excess source was derived from lateral or downslope transport of high ^{210}Pb activity fine-grained sediments. Narita *et al.* (1990) also reported that a large fraction of deeper settling particles collected in a short period (13 days) in the Okinawa Trough were transported laterally and downward through the near bottom determined by natural radionuclides. In fact, the deeper traps closer to the geographic boundary received heavier loads of particles, implying effects of resuspension and lateral transport. Furthermore, particle size distributions for

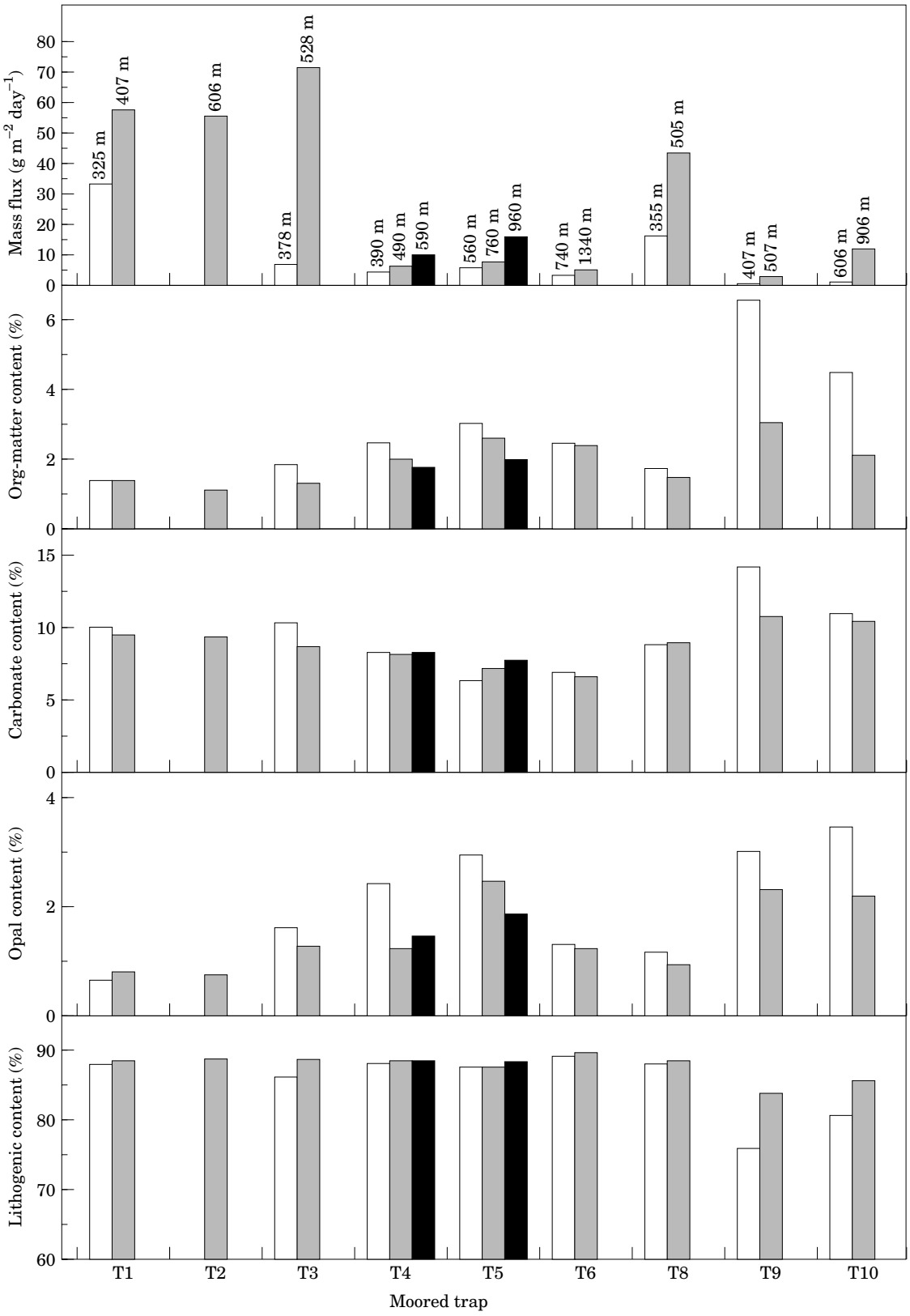

FIGURE 5. Variations of mass flux and major-component contents (organic matter, carbonate, opal and lithogenic material) for T1–T10 traps. Each data is a mean value averaged from those of successful cups.

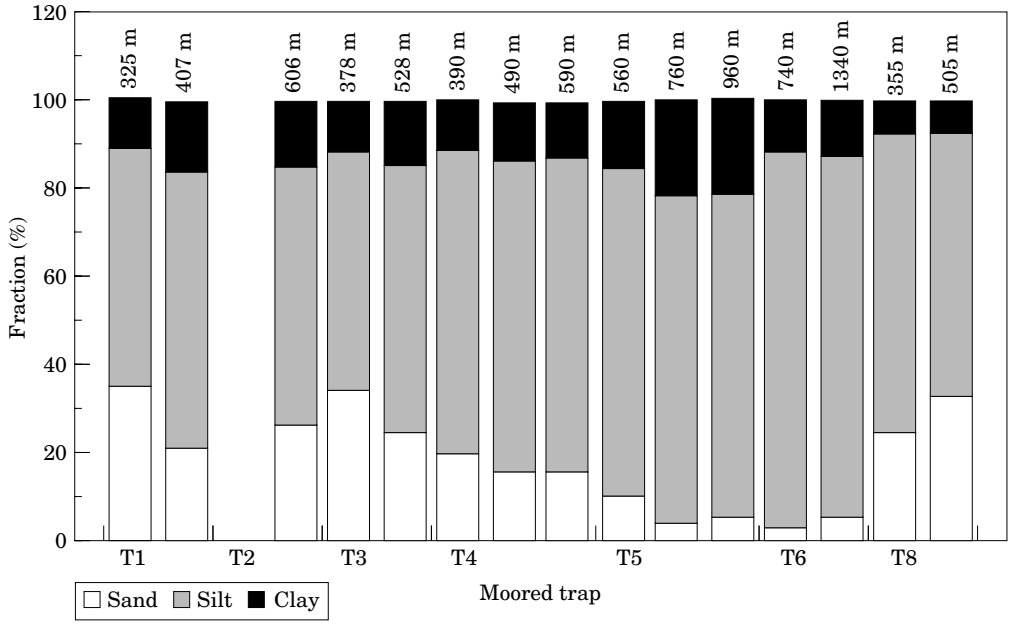

FIGURE 6. Particle-size distributions for T1–T10 traps. Each data is a mean value averaged from those of successful cups.

T1–T3 samples shown in Figure 6 (20–34% sand, 54–64% silt and 10–15% clay) are large difference from those of bottom sediments in the MHC area (6·0–7·5% sand, 35·4–47·3% silt and 45·2–58·6% clay) reported by Lin *et al.* (1992). This may suggest that traps do not collect particles resuspended directly from *in situ* sediment. Differential settling of large particles may occur during seaward transport of resuspended particles as reflected by the decrease of sand contents in T4–T6 samples (Figure 6). This resuspension coupling with lateral transport appears to be a conventional means of determining particle fluxes observed in various environments of continental margins (Biscaye *et al.*, 1988; Gardner, 1989; Monaco *et al.*, 1990; Pejrup *et al.*, 1996).

Spatial distributions of major-component fluxes vary coincidentally with those of mass fluxes because mass fluxes determine fluxes of major components exclusively (Table 3), although relative contents of major components do not co-vary with mass fluxes. Figure 5 indicates that contents of biogenic components (organic matter and opal) increase with a decrease of mass fluxes. Thus, mass flux correlates inversely with organic matter content ($r = -0{\cdot}5768$, $P<0{\cdot}01$) and opal content ($r = -0{\cdot}5652$, $P<0{\cdot}01$). According to data in Table 3, biogenic contents are generally lower in deeper TPM than in shallow TPM, which is possible attributed to the increase of decomposition with depth as well as from dilution by the heavy load of lithogenic materials that principally determine the extent of mass flux. Despite the comparable primary production between the southern ECS shelf (545 ± 167 mg C m^{-2} day^{-1}, Gong *et al.*, 1999) and the SEEP-I shelf (820 mg C m^{-2} day^{-1}, Falkowski *et al.*, 1994), a large difference was found for C_{org} content in TPM between this study (0·53–3·27%) and SEEP-I (4–17%, Biscaye *et al.*, 1988) and SEEP-II (2·6–14%, Biscaye & Anderson, 1994). Opal contents are also lower in our samples (0·67–3·5%) than in SEEP-II samples (5–20%, Biscaye & Anderson, 1994). The relatively low content of C_{org} in our TPM is apparently owing to dilution by laterally derived lithogenic materials. The vertical C_{org} flux out of euphotic layer is estimated to be 42 mg C m^{-2} day^{-1} if 285 mg C m^{-2} day^{-1} is applied for primary production (Gong *et al.*, 1999) and assume 0·15 for *F*-ratio in the slope area. The contribution of vertical C_{org} flux to trap C_{org} flux ranges from 8 to 34% (Table 5) for bottom traps (except for T9) under the assumption of settling velocity of 50 m day^{-1} [averaged from quickly settling (*c.* 100 m day^{-1}) and slowly sinking (*c.* 20 m day^{-1}) velocity] and exponential oxidation rate of 4% day^{-1} (Banse, 1990; Walsh, 1994). Lateral fluxes therefore contribute up to 66–92% of C_{org} fluxes measured in this study. The uncertainty may be large because the calculated values depend on assumed new production, settling velocity and oxidation rate. Carbonate may consist of both biogenic and terrigenous matter; therefore, its content does not correlate well with mass flux ($r = -0{\cdot}01$).

The lithogenic component in this study is expressed by the sum of aluminosilicate and non-aluminosilicate

TABLE 5. The contribution (%) of vertical C_{org} flux to total C_{org} fluxes collected from bottom traps

Trap sample	C_{org} content (%)	C_{org} flux (mg m^{-2} day^{-1})	Vertical contribution (%)
T1 (407 m, 83 mab)	0·675	365	8·1
T2 (606 m, 89 mab)	0·525	217	13
T3 (528 m, 50 mab)	0·629	368	8·3
T4 (590 m, 228 mab)	0·857	80	34
T5 (960 m, 100 mab)	0·982	100	20
T6 (1340 m, 100 mab)	1·181	58	26
T8 (505 m, 100 mab)	0·725	294	10
T9 (507 m, 100 mab)	1·514	36	81
T10 (906 m, 100 mab)	1·051	121	19

silicic detritus (e.g. quartz). Aluminosilicate content relative to the total mass ranges from 41·0–60·5% in T1–T3 (and T8) traps to 62·9–75·0% in T4–T6 traps, and from 54·3% to 74·6% in T9–T10 traps. Apparently, aluminosilicates (expressed as Al) present mainly in fine particles which correlate inversely with total mass fluxes ($r = -0{\cdot}5055$, $P<0{\cdot}05$). Aluminosilicates also correlate well with Fe, Mn, K and Mg which are generally regarded as terrigenous elements ($r \geq 0{\cdot}4348$, $P<0{\cdot}05$), which display consistent results for lithogenic dominance. Consequently, non-aluminosilicate silicic detritus which are much coarser, comprise 28·3–47·3% of total mass in T1–T3 (and T8) traps, 12·7–25·6% in T4–T6 traps and 8·3–27·4% in T9–T10 traps. Although the silicic content decreases with a decrease of mass flux, a significant extent is still collected by T6 traps located on the farthest distance from the shelf break. The silicic detritus collected by a trap is more likely derived from resuspension of local and/or remote sediments rather than directly from riverine inputs because of its relatively fast sinking property. Notably, quartz is predominant in non-aluminosilicate silicic detritus estimated qualitatively from x-ray diffraction pattern for T1 trap samples (data not shown here). Lithogenic fluxes below the surface layer constitute 76–90% (86–90% for T1–T8) of mass fluxes regardless of trap locations and depths. These results strongly suggest that particles collected by traps in this study area are largely terrigenous and transported laterally. Mien-Hwa canyon should be the major conduit in the transport of particles from the ECS shelf and slope to the Okinawa Trough basin.

Distributions of most lithogenic elements in T1–T10 samples listed in Table 4 provide another evidence for sediment resuspension and lateral transport in determining particle fluxes from the slope to the Okinawa Trough. Elemental contents also vary spatially, which are determined to a large extent by particle size distributions which, are ultimately influenced by mass fluxes referred from their significant correlations. Aluminium content is much lower in trap materials (3·38–6·17%) than in Yangtze (8·4%) and Yellow (7·5%) riverine SPM (Qu & Yan, 1990) and crustal average (8·23%; Taylor, 1964), resulting from the dilution of Al in trap materials by resuspended materials. Approximately 40–73% of trap materials may be roughly regarded as recent inputs from the Yangtze and/or Yellow Rivers derived from the fraction of TPM Al over the Yangtze particulate Al. The remaining portion (27–60%) of trap materials arises from biogenic and recycled contributions. Although the biogenic contribution can reach up to 10–24%, nearly two-thirds of them are derived from lateral transport (Lin, 1997). The recycled contribution is estimated to be 17–36%, which is comparable to the content of non-aluminosilicate silicic detritus that is an indicator of resuspension.

The contents of other major elements (Fe, Mn, Mg and K), similar to Al, are also lower in trap materials than in Yangtze and Yellow riverine SPM, as a result of dilution process. The ratios of these elements to aluminium, with a few exceptions, are close to the ratios in Yangtze and Yellow riverine SPM, indicating that no significant enrichment occurs during the long journey of most lithogenic elements. However, manganese contents and Mn/Al ratios are consistently higher in the lower trap than in the upper trap for all sites, which are attributed to the scavenging of dissolved Mn primarily transported laterally from the shelf or slope where dissolved Mn releases from suboxic/anoxic sediments. Minakawa *et al.* (1996) estimated that 14% of total deposited Mn in the ECS shelf floor was released into the water column through benthic flux. The lateral flux of dissolved Mn from the ECS shelf to the Okinawa Trough was further

estimated to be $(5 \pm 4) \times 10^5$ mol day^{-1} by using a box model (Minakawa *et al.*, 1996). It is worth noting that an exceptionally high Mn/Al value found in T6–1340 m may be attributed to the scavenging of upward flux of dissolved Mn from hydrothermal activity in the Okinawa Trough. Saito (1991, quoted from Minakawa *et al.*, 1996) also reported a high Mn/Al ratio ($6{\cdot}79 \times 10^{-2}$) of settling particles at 1390 m in the Okinawa Trough. Anomalously high dissolved Mn has been detected near the bottom of the Okinawa Trough by Ishibashi *et al.* (1988) and Wei *et al.* (1991) and they argued the influence of hydrothermal activity on Mn enrichment. Potassium is relatively enriched in all traps, which may be attributed to the contribution of potassium feldspar, as judged from the x-ray diffraction pattern of T1 TPM.

Temporal variability of mass flux and lithogenic composition

Figures 7 and 8 display the short-term variations of mass fluxes and lithogenic compositions for periods set for traps from the MHC (T1, T3) and deep slope (T6) of the Okinawa Trough. Temporal variations of SPM fluxes from the Yangtze River are also presented for comparison. Although T1 and T3 were deployed during different intervals, flux variations of two traps can be linked together to show variation for a longer period because two traps are geographically similar in the MHC. Mass fluxes [Figures 7(b)] apparently do not vary coincidentally with riverine fluxes [Figure 7(a)] during the periods of trap deployment. As chemical fluxes always follow mass fluxes, temporal variations of mass and chemical fluxes are not likely attributed to variability of riverine inputs, even though a time lag may exist between TPM fluxes and riverine fluxes. Local productivity, as aforementioned, contributes insignificantly to collected TPM and may not account for major variations of mass fluxes either. Temporal variations of aluminosilicate contents in TPM [Figure 7(c)] appear to follow the temporal trend of riverine fluxes [Figure 7(a)], largely because aluminosilicate is the major component of riverine SPM (Al: 8·4%, Qu & Yan, 1990). However, aluminosilicate contents almost vary inversely with TPM fluxes [Figure 7(b,c)]. In contrast, non-aluminosilicate silicic contents, an indication of resuspension, vary coincidentally with TPM fluxes [Figure 7(b,d)]. In order to maintain similar degree of TPM fluxes through T3 and T1 periods, the extent of resuspension must be greater in the T1-trap period than in the T3-trap period to compensate the decrease of riverine fluxes.

Although TPM fluxes do not correlate well with velocity and prevailing direction of measured current, high mass fluxes are essentially associated with large tidal current velocity oscillation observed in the MHC (Hung & Chung, 1998). Tsai (1996) also moored nephelometers and observed that the SPM flux is always higher when tidal current is eastward and argued that the tidal current is one of the major agents for transporting particles near the shelf break of this study area. The flux variation is still distinct for T4 site (figure is omitted for brevity sake) locating on the outlet of MHC where the mean current velocity is 20 cm s^{-1} at 390 m with a mass flux at 4·04 g m^{-2} day^{-1} and 10 cm s^{-1} at 590 m with a mass flux at 9·90 g m^{-2} day^{-1}. Apparently, current velocity does not determine the temporal variations of TPM fluxes.

Both flux extent and flux fluctuation are obviously reduced based on the same time scale for T6 (Figure 8) where the mean current velocity also decreases to 3–5 cm s^{-1} between 740 and 1340 m. Meanwhile, the influence of tidal fluctuation on particle flux may become negligible below 740 m. Notably, the lithogenic flux continues to play a dominant role in determining total mass flux for T6 located on the farthest distance from the shelf break, although the mass flux [Figure 8(b)] is unlikely constrained by the riverine flux [Figure 8(a)]. On the other hand, the non-aluminosilicate silicic content is <30% [Figure 8(d)] and becomes less critical in determining TPM flux [Figure 8(b)], possibly owing to a longer travelling distance for resuspended particles. Nevertheless, episodic events of sediment resuspension coupled with lateral transport may be responsible for such a great temporal fluctuation of TPM fluxes.

Conclusion

Several lines of evidence support the notion that the processes of resuspension and lateral transport from shelf/slope sediments, to a large extent, determine SPM distributions and TPM fluxes over the study area. Such evidence includes (i) horizontal decrease and vertical increase of SPM and particulate Al, Fe and Mn distributions in the southern East China Sea; (ii) the presence of intermediate-layer plume for SPM, particulate Al and relatively old C_{org} in the Okinawa Trough overlying the Kuroshio water; (iii) TPM is mainly lithogenic, the fluxes of total mass and lithogenic materials decrease horizontally and increase vertically regardless of trap sites; (iv) vertical fluxes may contribute <34% of C_{org} collected from bottom traps; and (v) non-aluminosilicate silicic

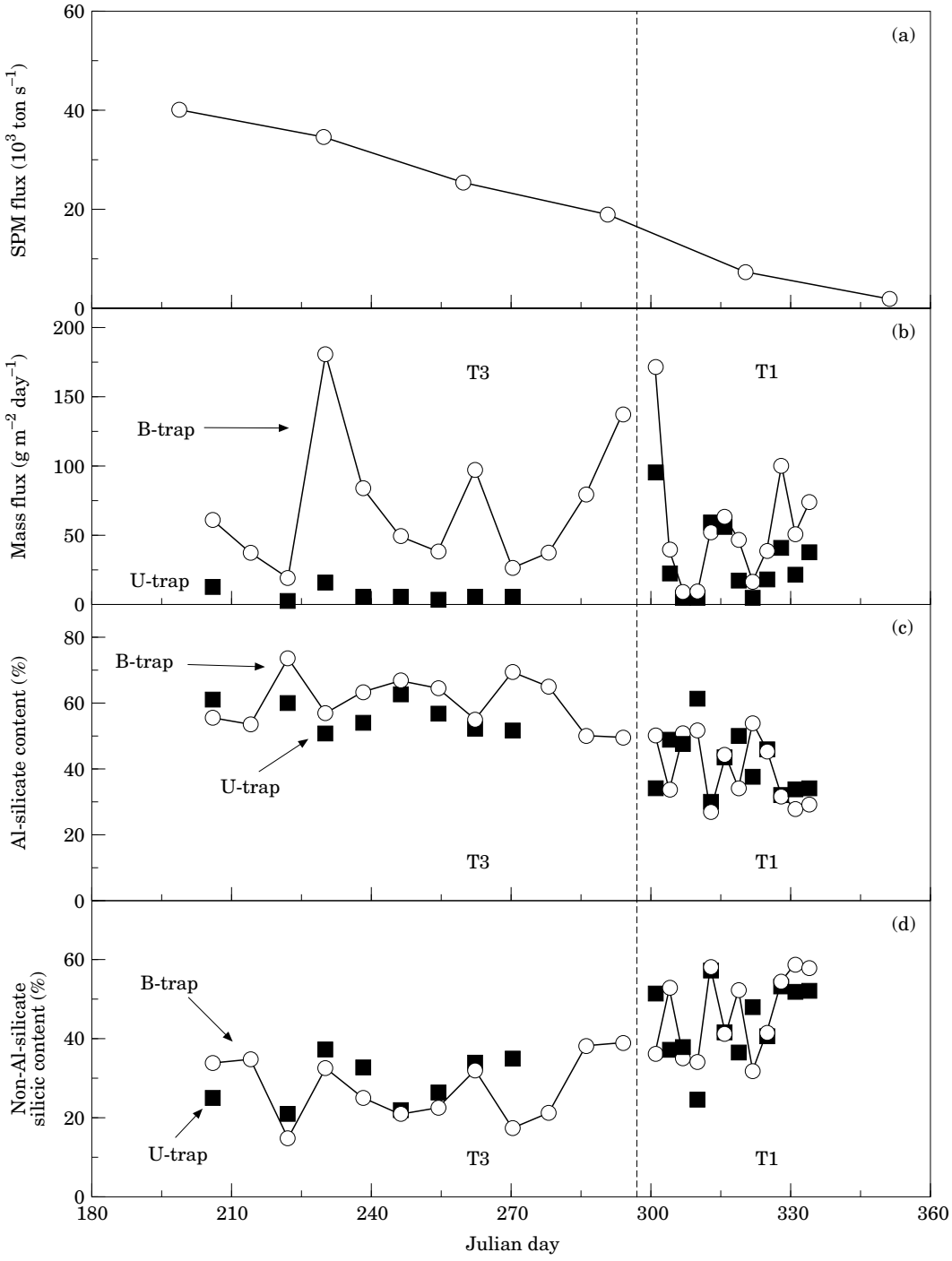

FIGURE 7. Comparison of temporal variations between (a) SPM fluxes from the Yangtze River (data from Milliman *et al.*, 1984) and (b–d) mass fluxes, aluminosilicate contents and non-aluminosilicate silicic contents from T1 and T3 traps.

detritus contribute significantly to the mass flux for most traps. TPM fluxes are markedly high within the MHC; the fluxes may be the highest among observations from worldwide continental margins. Thus, MHC appears to be the most essential conduit for particle transport from the southern ECS shelf to the Okinawa Trough. Finally, short-term variabilities of mass and lithogenic fluxes may arise primarily from episodic events of sediment resuspension/detachment and lateral transport, rather than from temporal variations of riverine inputs and local production.

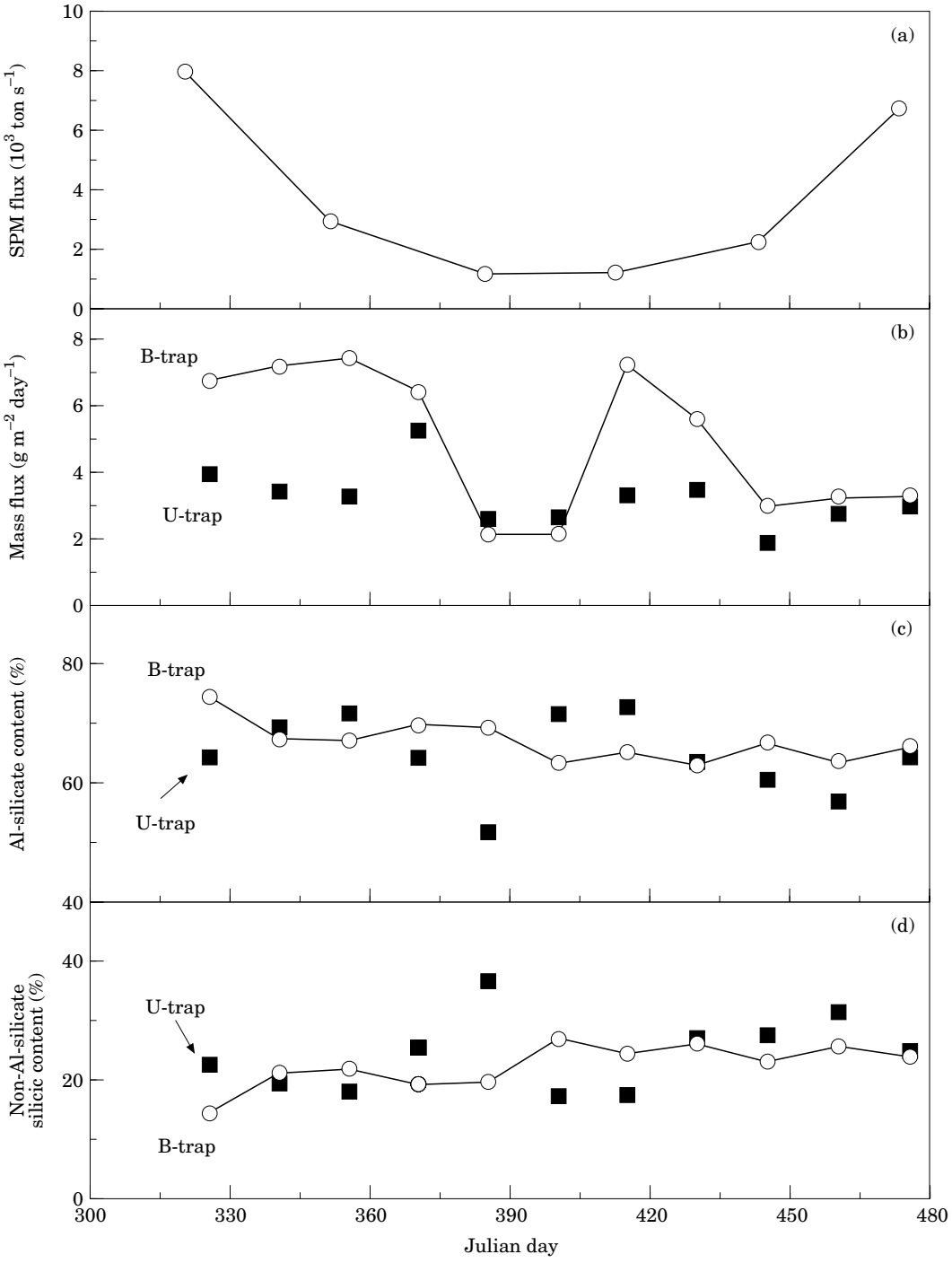

FIGURE 8. Comparison of temporal variations between (a) SPM fluxes from the Yangtze River (data from Milliman *et al.*, 1984) and (b–d) mass fluxes, aluminosilicate contents and non-aluminosilicate silicic contents from T6 trap.

Acknowledgements

The authors would like to thank National Science Council, Republic of China for financially supporting this research under Contract Nos. NSC 83-0209-M110-009k, NSC 84-2611-M110-006k2, and NSC 85-2611-M110-010-k2. The captain, crew and research assistants aboard the RV *Ocean Researcher I* and *II* are appreciated for technical support and sampling assistance during deployments and

recoveries of sediment traps. We are also grateful to anonymous reviewers for constructive comments on the manuscript. This research is a contribution to the KEEP (Kuroshio Edge Exchange Process) study, a recognized program of the JGOFS.

References

Baker, E. T. 1976 Distribution, composition and transport of suspended particulate matter in the vicinity of Willapa, Submarine Canyon, Washington. *Geological Society of American Bulletin* **87,** 625–632.

Baker, E. T. & Hickey, B. M. 1986 Contemporary sedimentation processes in and around an active west coast submarine canyon. *Marine Geology* **71,** 15–34.

Banse, K. 1990 New views on the degradation and disposition of organic particles as collected by sediment traps in the open sea. *Deep-Sea Research* **37,** 1177–1195.

Biscaye, P. E., Anderson, R. F. & Deck, B. L. 1988 Fluxes of particles and constituents to the eastern United States continental slope and rise. *Continental Shelf Research* **8,** 855–904.

Biscaye, P. E. & Anderson, R. F. 1994 Fluxes of particulate matter on the slope of the southern Middle Atlantic Bight: SEEP-II. *Deep-Sea Research II* **41,** 459–509.

Chao, S.-Y. 1991 Circulation of the East China Sea: a numerical study. *Journal of Japanese Oceanographic Society* **46,** 273–295.

Chern, C. S., Wong, J. & Wong, D. P. 1990 The exchange of Kuroshio and East China Sea shelf water. *Journal of Geophysical Research* **95,** 16017–16023.

Chin, Y.-S. 1979 A study on sediment and mineral compositions [sic] of the sea floor of the East China Sea. *Ocean Sciences* **2,** 130–142.

Chung, W. S., Li, H. W., Tang, T. Y. & Wu, C. K. 1993 Observations of the countercurrent on the inshore side of the Kuroshio northeast of Taiwan. *Journal of Oceanography* **49,** 581–592.

Chung, Y. & Chang, W. C. 1995 Pb-210 fluxes and sedimentation rates on the lower continental slope between Taiwan and the South Okinawa Trough. *Continental Shelf Research* **15,** 149–164.

Drake, D. E. 1974 Distribution and transport of suspended particulate matter in submarine canyon off Southern California. In *Suspended Solids in Water* (Gibbs, R. J., ed.) Plenum Press, New York, pp. 133–153.

Falkowski, P. G., Biscaye, P. E. & Sancetta, C. 1994 The lateral flux of biogenic particles from the eastern North American continental margin to the North Atlantic Ocean. *Deep-Sea Research II* **41,** 583–601.

Gardner, W. D. 1989 Baltimore canyon as a modern conduit of sediment to the deep sea. *Deep-Sea Research* **36,** 323–358.

Gong, G.-C., Chang, J. & Wen, Y. H. 1999 Estimation of annual primary production in the Kuroshio waters northeast of Taiwan using a photosynthesis-irradiance model. *Deep-Sea Research I* **46,** 93–108.

Gordon, D. C. 1970 Some studies of the distribution and composition of particulate organic carbon in the North Atlantic Ocean. *Deep-Sea Research* **17,** 233–243.

Heussner, S., Ratti, C. & Carbonne, J. 1990 The PPS 3 time-series sediment trap and the trap sample processing techniques used during the ECOMARGE experiment. *Continental Shelf Research* **10,** 943–958.

Hsiung, T. M., Gong, G. C. & Pai, S. C. 1998 A persistent mid-depth dissolved manganese maximum in the southern Okinawa Trough. *Terrestrial, Atmospheric and Oceanic Sciences* **9,** 119–125.

Hsueh, Y., Chern, C. S. & Wong, J. 1992 The intrusion of Kuroshio across the continental slope northeast of Taiwan. *Journal of Geophysical Research* **97,** 14323–14330.

Hung, G. W. & Chung, Y. 1998 Particulate fluxes, Pb-210 and Po-210 measured from sediment trap samples in a canyon off northeast Taiwan. *Continental Shelf Research* **18,** 1475–1498.

Hung, J. J. & Chan, C. L. 1998 Distribution and enrichment of particulate trace metals in the southern East China Sea. *Geochemical Journal* **32,** 189–203.

Ishibashi, J.-I., Gamo, T., Sakai, H., Nojiri, Y., Igarashi, G., Shitashima, K. & Tsubota, H. 1988 Geochemical evidence for hydrothermal activity in the Okinawa Trough. *Geochemical Journal* **22,** 107–114.

Jan, S. 1995 *Seasonal variations of currents in the Taiwan strait*. Ph.D. Thesis, Institute of Oceanography, National Taiwan University, 139 pp.

Leinen, M. 1977 A normative calculation technique for determining opal in deep-sea sediments. *Geochimica et Cosmochimica Acta* **41,** 671–676.

Li, Y.-H. 1994 Material exchange between the East China Sea and the Kuroshio current. *Terrestrial, Atmospheric and Oceanic Sciences* **5,** 625–631.

Lin, C. S. 1997 *Fluxes of Particles and Chemical Constituents in the Southern East China Sea Northeast of Taiwan*. M.S. Thesis, National Sun Yat-Sen University, Taiwan, 88 pp.

Lin, S., Liu, K. K., Chen, M. P., Chen, P. & Chang, F. Y. 1992 Distribution of organic carbon in the KEEP area continental margin sediments. *Terrestrial, Atmospheric and Oceanic Sciences* **3,** 365–378.

Liu, K. K., Gong, G. C., Lin, S. W., Yang, C. Y., Wei, C. L., Pai, S. C. & Wu, C. K. 1992 The year-round upwelling at the shelf break near the northern tip of Taiwan as evidenced by chemical hydrography. *Terrestrial, Atmospheric and Oceanic Sciences* **3,** 243–276.

Milliman, J. D. & Meade, R. H. 1983 World wide delivery of river sediment to the oceans. *Journal of Geology* **91,** 1–21.

Milliman, J. D., Shen, H. T., Yang, Z. S. & Meade, R. H. 1985 Transport and deposition of river sediment in Changjiang estuary and adjacent continental shelf. *Continental Shelf Research* **4,** 37–45.

Milliman, J. D., Xie, Q. & Yang, Z. 1984 Transfer of organic carbon and nitrogen from the Yangtze River to the ocean. *American Journal of Science* **284,** 824–834.

Minakawa, M., Noriki, S. & Tsunogai, S. 1996 Manganese in the East China Sea and the Yellow Sea. *Geochemical Journal* **30,** 41–55.

Monaco, A., Biscaye, P. E., Soyer, J., Pocklington, R. & Heussner, S. 1990 Particle fluxes and ecosystem response on a continental margin: the 1985–1988 Mediterranean ECOMARGE experiment. *Continental Shelf Research* **10,** 809–839.

Mortlock, R. A. & Froelich, P. N. 1989 A simple method for the rapid determination of biogenic opal in pelagic marine sediments. *Deep-Sea Research* **36,** 1415–1426.

Narita, H., Harada, K. & Tsunogai, S. 1990 Lateral transport of sediment particles in the Okinawa Trough determined by natural radionuclides. *Geochemical Journal* **24,** 207–216.

Nitani, H. 1972 The beginning of the Kuroshio. In *Kuroshio* (Stommel, H. & Yoshida, K., eds). University of Tokyo Press, Japan, pp. 129–156.

Pejrup, M., Valeur, J. & Jensen, A. 1996 Vertical fluxes of particulate matter in Aarhus Bight, Denmark. *Continental Shelf Research* **16,** 1047–1064.

Qu, C. & Yan, R. 1990 Chemical composition and factors controlling suspended matter in three major Chinese rivers. *The Science of Total Environment* **97/98,** 335–346.

Saito, C. 1991 *Characteristic of chemical substances in the ocean studied with sediment trap*. Ph.D. Thesis, Hokkaido University, 65 pp. (in Japanese).

Sherrell, R. M., Field, M. P. & Gao, Y. 1998 Temporal variability of suspended mass and composition in the Northeast Pacific water column: relationships to sinking flux and lateral advection. *Deep-Sea Research II* **45,** 733–761.

Sternberg, R. W., Larsen, L. H. & Miao, Y. T. 1985 Tidally driven sediment transport on the East China Sea continental shelf. *Continental Shelf Research* **4,** 105–120.

Tang, T. Y., Hsueh, Y., Yang, Y. J. & Ma, J. C. 1999 Continental slope flow northeast of Taiwan. *Journal of Physical Oceanography* (in press).

Taylor, S. R. 1964 Abundance of chemical elements in the continental crust: a new table. *Geochimica et Cosmochimica Acta* **28,** 1273–1285.

Thorbjarnarson, K. W., Nittrouer, C. A. & DeMaster, D. J. 1986 Accumulation of modern sediment in Quinault submarine canyon. *Marine Geology* **71,** 107–124.

Tsai, C. H. 1996 An assessment of a time-to-transition lazer sizer in measuring suspended particles in the ocean. *Marine Geology* **134,** 95–112.

Walsh, J. J. 1994 Particle export at Cape Hatteras. *Deep-Sea Research II* **41,** 603–628.

Wei, C. L., Sun, S. J. & Huang, C. S. 1991 Manganese distribution in the water column off northeast Taiwan—A preliminary investigation. *Acta Oceanographica Taiwanica* **26,** 85–93.